

Heralded Three-Photon Entanglement from a Single-Photon Source on a Photonic Chip

Si Chen^{1,2,3}, Li-Chao Peng^{1,2,3}, Y.-P. Guo^{1,2,3}, X.-M. Gu^{1,2,3}, X. Ding^{1,2,3}, R.-Z. Liu^{1,2,3}, J.-Y. Zhao^{1,2,3},
 X. You^{1,2,3,4}, J. Qin^{1,2,3}, Y.-F. Wang^{1,2,3}, Yu-Ming He^{1,2,3}, Jelmer J. Renema^{5,*}, Yong-Heng Huo^{1,2,3,†},
 Hui Wang^{1,2,3,‡}, Chao-Yang Lu^{1,2,3} and Jian-Wei Pan^{1,2,3,§}

¹*Hefei National Research Center for Physical Sciences at the Microscale and School of Physical Sciences, University of Science and Technology of China, Hefei 230026, China*

²*Shanghai Research Center for Quantum Science and CAS Center for Excellence in Quantum Information and Quantum Physics, University of Science and Technology of China, Shanghai 201315, China*

³*Hefei National Laboratory, University of Science and Technology of China, Hefei 230088, China*

⁴*University of Science and Technology of China, School of Cyberspace Security, Hefei, China*

⁵*QuiX Quantum B.V., Hengelosestraat 500, 7521 AN Enschede, The Netherlands*



(Received 30 June 2023; accepted 22 February 2024; published 28 March 2024)

In the quest to build general-purpose photonic quantum computers, fusion-based quantum computation has risen to prominence as a promising strategy. This model allows a ballistic construction of large cluster states which are universal for quantum computation, in a scalable and loss-tolerant way without feed forward, by fusing many small n -photon entangled resource states. However, a key obstacle to this architecture lies in efficiently generating the required essential resource states on photonic chips. One such critical seed state that has not yet been achieved is the heralded three-photon Greenberger-Horne-Zeilinger (3-GHZ) state. Here, we address this elementary resource gap, by reporting the first experimental realization of a heralded 3-GHZ state. Our implementation employs a low-loss and fully programmable photonic chip that manipulates six indistinguishable single photons of wavelengths in the telecommunication regime. Conditional on the heralding detection, we obtain the desired 3-GHZ state with a fidelity 0.573 ± 0.024 . Our Letter marks an important step for the future fault-tolerant photonic quantum computing, leading to the acceleration of building a large-scale optical quantum computer.

DOI: [10.1103/PhysRevLett.132.130603](https://doi.org/10.1103/PhysRevLett.132.130603)

The photon is a favorable candidate for universal quantum computing [1–3], allowing several advantages such as room-temperature operation, negligible decoherence, and easy integration into existing fiber-optic-based telecommunications systems. Especially, the rapidly developed integrated optics makes it an appealing physical platform for large-scale fault-tolerant quantum computing [4–6].

Measurement-based quantum computing (MBQC) [7–10], where quantum algorithms are performed by making single qubit measurements on a large entangled state—usually called cluster states, holds significant potential for photonic systems based on linear optics. Large-scale cluster states can be efficiently created from small resource states in a fusion mechanism [11,12]. Later, a ballistic strategy for MBQC has been proposed [13–16], enabling scalable and loss-tolerant generation of large cluster states by fusing many small entangled resource states without any feed forward, which has subsequently renormalized to fusion-based quantum computation [17]. Currently, one of the key challenges for scalable MBQC is the efficient generation of the necessary small resource clusters.

Deterministic generations of multiphoton cluster states from single quantum emitters have been proposed [18–20]

and implemented [21–24]. However, high-quality deterministic preparation still remains challenging with existing technologies. Alternatively, entangled clusters can be near-deterministically generated in a heralded manner, allowing immediate awareness of success without destroying the target state. The pioneering realization of heralded single photons was first accomplished by Hong and Mandel in 1986 [25]. Over a span of 24 years, sustained effort led to the successful creation of the first heralded entangled photon pairs, achieved with the use of three EPR pairs [26,27]. Despite these advancements, it is crucial to note that neither heralded single photons nor heralded entangled photon pairs can be directly utilized for fusion-based quantum computing in the absence of deterministic controlled-NOT gates. The heralded 3-GHZ state has been identified as the minimal initial entangled state [17], serving as an essential building block for constructing large entangled cluster states. Unfortunately, this state has remained unrealized, largely attributable to the shortage of high-efficiency quantum light sources.

Here, we report the first experimental demonstration of a heralded 3-GHZ state using six single photons [28,29] manipulated in a photonic chip. A high-quality single-photon source based on a semiconductor quantum dot [30]

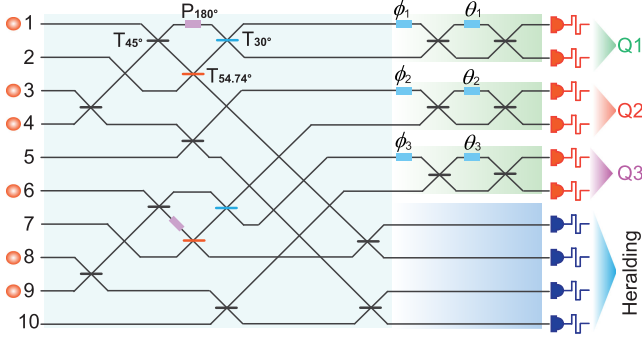


FIG. 1. The heralded generation scheme for a 3-GHZ state. Six single photons are prepared at the input ports of a linear optical circuit, where we can describe the initial input quantum state as $|\psi_{\text{in}}\rangle = |1011010110\rangle$ with 0 and 1 being the number of photons in each mode. The photonic circuit (depicted in the light cyan background color), which contains twelve beams splitters of three different transmissions— $1/2$ (black), $1/4$ (blue), $2/3$ (orange), and two π -phase shifters (purple)—implements a required unitary transformation U for a 3-GHZ state. The 3-GHZ state in dual-rail encodings (a single photon appearing in only one of the two spatial modes describes a qubit such as Q_1 , Q_2 , and Q_3) is heralded in the modes (1–6) by a measurement pattern in the last four modes (7–10). Three phase-tunable Mach-Zehnder interferometers of phases ϕ_i and θ_i ($i = 1, 2, 3$) are used to perform quantum state measurements on the created GHZ state.

embedded in an open microcavity is used to deterministically produce single photons that are converted to the telecommunication band with a quantum frequency converter [31,32]. These single photons are deterministically demultiplexed into six indistinguishable single-photon sources [33,34], which are manipulated in a fully programmable photonic chip [35]. Heralded by the detection of four output spatial modes with high-efficiency single-photon detectors, we obtain a heralded 3-GHZ state with a fidelity of 0.573 ± 0.024 . Our Letter is an important step towards fault-tolerant scalable photonic quantum computation.

Figure 1 illustrates a heralded generation of a dual-rail-encoded 3-GHZ state out of six single photons [29]. The scheme exploits a ten-mode linear optical circuit, which consists of twelve optical beams splitters with three distinct transmission coefficients and a pair of π -phase shifters. Six photons are injected into six specific input modes of the photonic circuit, preparing a number-basis initial state represented as $|\psi_{\text{in}}\rangle = a_1^\dagger a_3^\dagger a_4^\dagger a_6^\dagger a_8^\dagger a_9^\dagger |0\rangle^{\otimes 10} = |1011010110\rangle$. Here, a_i^\dagger refers to the creation operator in mode i , $|0\rangle$ symbolizes the vacuum state, and the numbers 0 and 1 indicate the number of photons occupied in each mode. The underlying unitary transformation U of the circuit is optimally parametrized such that particular measurement patterns in four ancillary modes (7–10) herald a desired 3-GHZ state at six output modes (1–6) [29]. Qubits Q_1 , Q_2 , and Q_3 are identified with output

mode pairs (1,2), (3,4), and (5,6). This association uses a dual-rail encoding method, which signifies the presence of one single photon in either of the two spatial modes within each mode pair, e.g., $|0\rangle_d = |10\rangle$ and $|1\rangle_d = |01\rangle$. The GHZ state is heralded in modes (1–6) only when single photons are detected in both (7,8) and in just one of the (9,10) ports, with the other one remaining in a vacuum state. Each event has a success probability of $1/108$, resulting in an overall success rate of $1/54$ [29]. Using phase-tunable Mach-Zehnder interferometers (MZIs) at each output mode pair, one can perform arbitrary local projective measurements for estimating the full state. Details of the underlying state evolution and state measurements are provided in Supplemental Material [36].

To prepare six single photons, we firstly use the state-of-the-art self-assembled InAs/GaAs quantum dot (QD), which is coupled to a polarized [41] and tunable microcavity [42] and cooled down to ~ 4 K. Under resonant pumping by a π -pulse laser with a repetition rate of ~ 76 MHz, the QD emits ~ 50 MHz polarized resonance fluorescence single photons at the end of the single-mode fiber. We measured the second-order correlation of the photon source with a Hanbury Brown–Twiss (HBT) interferometer [43], and obtained $g^2(0) = 0.028(8)$ at zero delay, which indicates a high single-photon purity of 97.2(8)%. The single photon indistinguishability is tested using a Hong-Ou-Mandel (HOM) interferometer [44], yielding a visibility of 89(1)% between two photons separated by ~ 13 ns.

We then employ a quantum frequency converter (QFC) to transfer the near-infrared wavelength of the produced single photons to the preferable telecommunication regime [32]. For this purpose, we fabricate a periodically poled lithium niobate (PPLN) waveguide for difference-frequency generation process that can be adjusted by the wavelengths of the pump lasers. A continuous wave (cw) pump laser at ~ 2060 nm and the QD-emitted single photons at ~ 884.5 nm are then coupled into the PPLN waveguide, in which the difference frequency generation occurs, thus generating the output single photons at 1550 nm. By optimizing the waveguide coupling, and transmission and detection rate, we eventually achieve an overall single-photon conversion efficiency of $\sim 50\%$. To test whether the converted photons still preserve the single-photon nature and their indistinguishability, we perform the HBT and HOM measurements on the photons after conversion. The purity of the single photons at 1550 nm stays 97.4(6)%, and the indistinguishability between photon 1 and photons 2, 3, 4, 5, 6 are, respectively, 0.883(7), 0.86(1), 0.86(3), 0.88(1), 0.87(3), as shown in Figs. 3(a) and 3(b).

The converted single-photon stream is then deterministically demultiplexed into six spatial modes using a treelike structure demultiplexer constructed by five pairs of Pockels cells (PCs) and polarizing beam splitters (PBSs). The PCs, synchronized to the laser pulses and operated at a

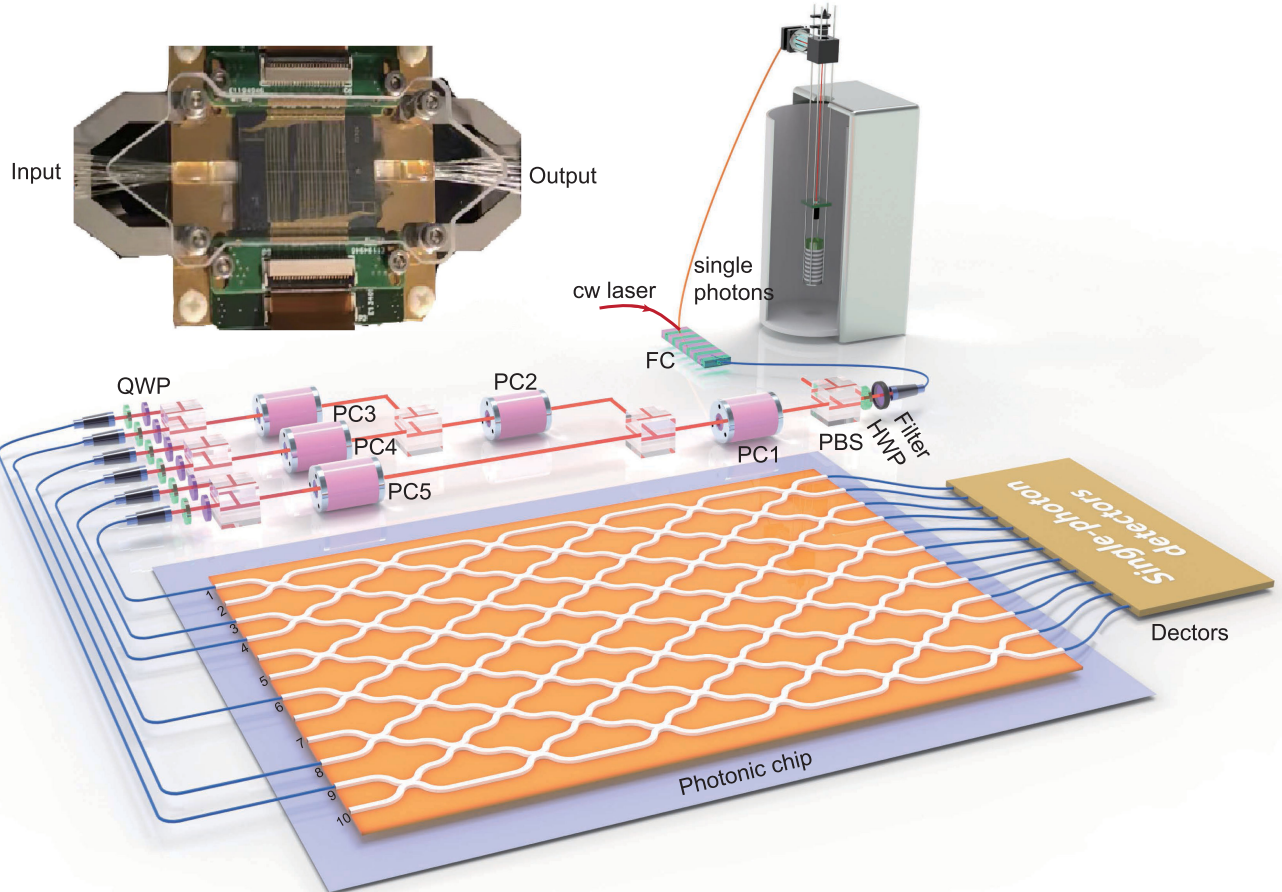


FIG. 2. The experimental setup. A single InAs/GaAs quantum dot, resonantly coupled to an open microcavity, is used to produce pulsed resonance fluorescence single photons. The wavelength of these single photons in near infrared is then converted into a telecom wavelength of 1550 nm with a quantum frequency converter by coupling a continuous wave laser and single photons into a periodically poled lithium niobate waveguide. Five pairs of Pockels cells and polarizing beam splitters are employed to actively translate a stream of single photons into six spatial modes. Optical fibers of different lengths are used to precisely compensate time delays. The six indistinguishable single photons are then fed into a 12-modes programmable linear-optical quantum circuit, which allows the preparation and measurement of a heralded three-qubit dual-rail encoded GHZ state. The single photons at the output ports of the photonic circuit are detected by superconducting nanowire single-photon detectors. All coincidences are recorded by a coincidence count unit (not shown).

repetition rate of ~ 705 kHz, actively control the photon polarization when loaded with high-voltage electrical pulses. The measured average optical switches efficiency is $\sim 77\%$, which is mainly due to the coupling efficiency and propagation loss. With the help of six single-mode fibers of different lengths and translation stages, we precisely compensate the relative time delays of the six single photons such that they can simultaneously arrive at the input ports of the photonic circuit.

To realize the functional design of the unitary transformation in Fig. 1, we employ a photonic chip that is low loss and fully programmable [35]. The circuit is based on stoichiometric silicon nitride waveguides which are fabricated for single-mode operation at telecom c band. It consists 12 input and output spatial modes that are interconnected through an arrangement of adjustable beam splitters and thermo-optic phase shifters, as shown in Fig. 2

(for details about the photonic circuit, please refer to Ref. [35]). To achieve a heralded 3-GHZ state, six single photons are injected into six inputs (1, 3, 4, 6, 8, 9) of the circuit and propagate through the circuit. The heralded outputs are 7, 8, 9, and 10. At each heralded output (7, 8, 9), two superconducting nanowire single-photon detectors (SNSPDs) are employed and act as a pseudo-photon-number detector that can resolve up to two photons. When each mode (7, 8, 9) contains a single photon and mode 10 has vacuum state, one can obtain a heralded GHZ generation for three dual-rail encoded qubits defined in the modes $Q1 = (1, 2)$, $Q2 = (3, 4)$, and $Q3 = (5, 6)$.

We then send the six photons one by one and measure the output distribution at the nine output modes (1–9) for analyzing the quality of the photonic circuit. For each input-output combination, we implement a Mach-Zehnder-type coherence measurement to record the corresponding

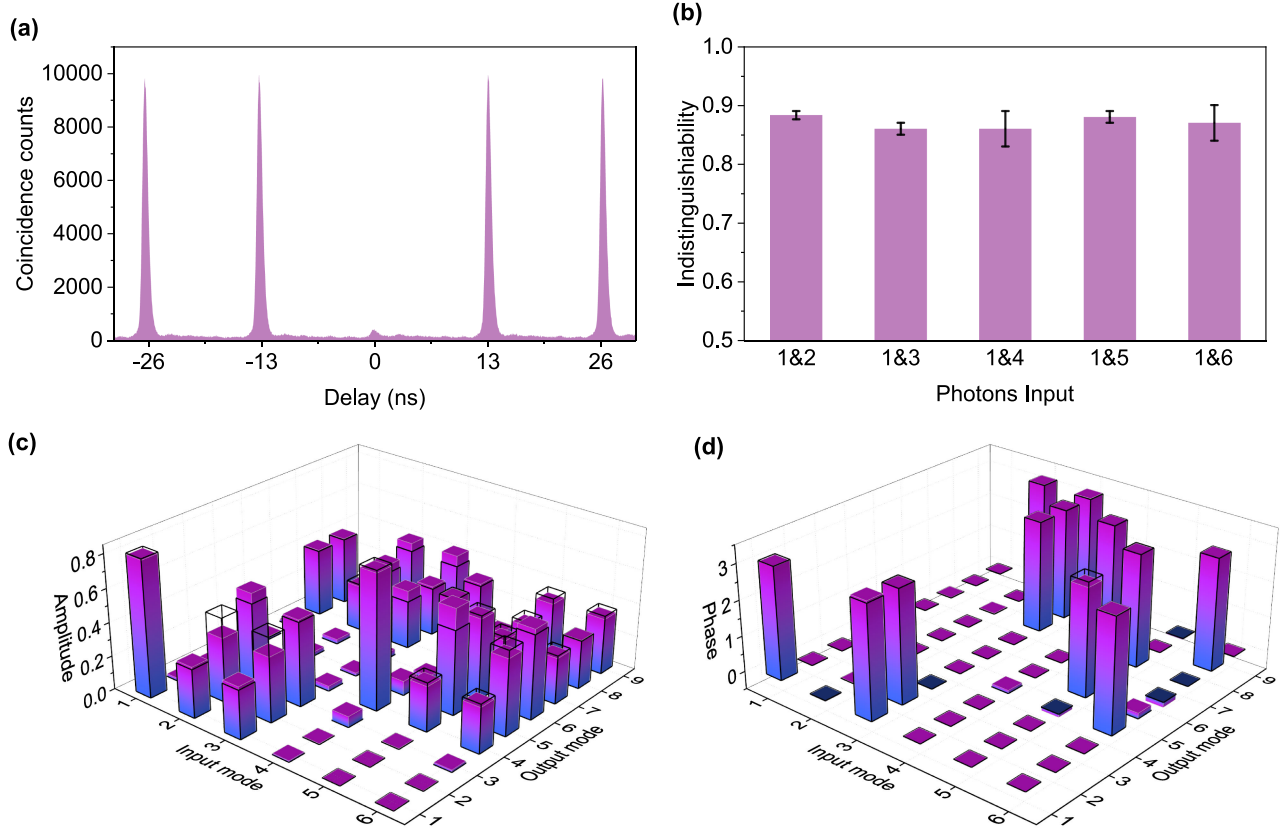


FIG. 3. Characterization of the single-photon source and the photonic quantum circuit. (a) The purity of the single-photon source of telecom wavelength is evaluated by a second-order correlation function $g^2(0)$. The observed antibunched peak at zero-time delay reveals $g^2(0) = 0.026(6)$. (b) Measurement of the photon indistinguishability by performing a Hong-Ou-Mandel interferometer between photon 1 and photon 2 (3, 4, 5, or 6). The corresponding measured indistinguishabilities are 0.883(7), 0.86(1), 0.86(3), 0.88(1), 0.87(3), respectively. The error bars indicates 1 standard deviation, deduced from propagated Poissonian counting statistics of the raw photon detection events. (c)–(d) Amplitude (c) and phase (d) of the ideal unitary transformation matrix (black wire frames) and their experimental reconstructions (colored bars). We send six single photons into the used six input ports of the photonic circuit, and measure the normalized amplitude and phase for each input-output combination.

phase. The normalized amplitude and measured phases compared to their theoretical distributions are summarized in Figs. 3(c) and 3(d).

To analyze the generated heralded three-photon GHZ state in dual-rail encoding, we use the phase-tunable MZIs to perform any local projective measurements on the single photons. The transformation matrixes of these local measurements are compiled in the whole circuit. We then collect the six-photon coincidence counts at the used ten outputs in which each output mode (7, 8, 9) contains only one photon. To validate the three-qubit GHZ entanglement, we first measure the six-photon events in the $|0\rangle_d/|1\rangle_d$ basis [see data in Fig. 4(a)] to calculate the population of $(|0\rangle_d\langle 0|_d)^{\otimes 3} + (|1\rangle_d\langle 1|_d)^{\otimes 3}$ over all the possible 2^3 combinations, leading to a population $P = 0.758 \pm 0.025$. We further estimate the expectation value of the observable $M_\theta^{\otimes N} = (\cos \theta \hat{\sigma}_x + \sin \theta \hat{\sigma}_y)^{\otimes N}$, where $\theta = k\pi/3$ ($k = 0, 1, 2$) and $\hat{\sigma}_x, \hat{\sigma}_y$ are Pauli matrices. The coherence of the three-qubit GHZ state is defined by the off-diagonal element of its density matrix and can be calculated by

$C = (1/3) \sum_{k=0}^2 (-1)^k \langle M_{k\pi/3}^{\otimes 3} \rangle$, which is $C = 0.389 \pm 0.040$ [see data in Fig. 4(b)]. The state fidelity can be directly estimated by $F = (P + C)/2 = 0.573 \pm 0.024$, which surpasses the classical threshold of 0.5 by more than 3 standard deviations and is sufficient to show the presence of entanglement [45].

In summary, we have demonstrated, for the first time, the heralded three-photon GHZ states using six photons from a high-quality quantum-dot single-photon source and a 12-mode fully programmable photonic chip. It should be noted that this experiment is unrealistic for commonly used spontaneous parametric down-conversion sources [46], since the expected count rate will be 4 orders of magnitude smaller than this experiment, showing a huge advantage of deterministic quantum-dot single-photon sources. Our demonstrated three-qubit GHZ state is heralded and has a heralding efficiency that could reach to 1 in principle, which is the main building block for fusion-based photonic quantum computing. Here, the heralding efficiency is defined as the probability of successfully achieving a desired

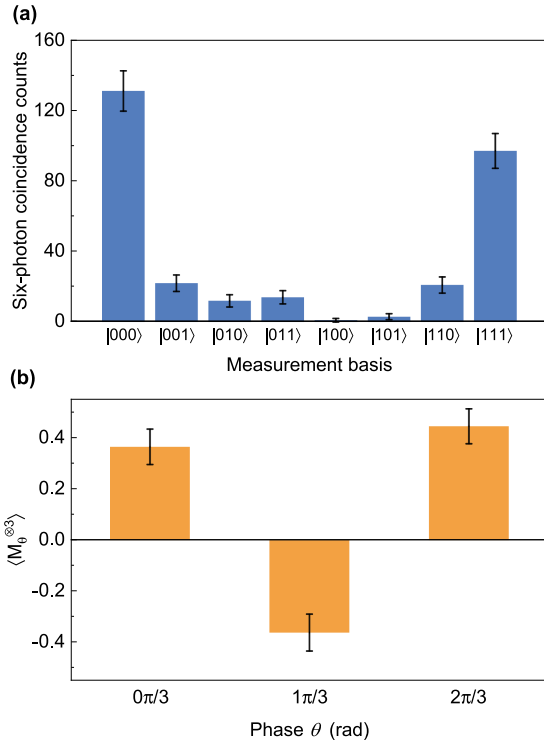


FIG. 4. Experimental results of the generated heralded three-qubit GHZ state. (a) Six-photon coincidence counts measured in the dual-rail basis $|0\rangle_d/|1\rangle_d$ accumulated for 23 h. (b) Expectation values of $\langle M_\theta^{\otimes 3} \rangle$ with phase shift being $\theta = k\pi/3$ ($k = 0, 1, 2$), each obtained from the measurement in the basis of $(|0\rangle_d \pm e^{i\theta}|1\rangle_d)/\sqrt{2}$. Error bars indicate 1 standard deviation calculated from Poissonian counting statistics of the raw detection events.

GHZ state when there are coincidences of desired heralding detectors. In our experiment, we obtain a heralding efficiency of ~ 0.0005 after the correction of imperfections of the detector (see Supplemental Material [36]). This heralding efficiency can be significantly improved in the near future by further promoting the efficiency of single-photon sources and the photonic circuit to enable large-scale photonic quantum computing.

Note added.—Recently, we became aware of a related work [47]. During the process of review, we noticed another related work [48].

This work was supported by the National Natural Science Foundation of China, the National Key R&D Program of China (No. 2019YFA0308700), the Chinese Academy of Sciences, the Anhui Initiative in Quantum Information Technologies, and the Science and Technology Commission of Shanghai Municipality (No. 2019SHZDZX01). Innovation Program for Quantum Science and Technology (No. ZD0202010000), and the New Cornerstone Science Foundation. The authors would like to thank J. Epping, M. de Goede, H. Snijders,

P. Venderbosch, B. Kassenberg and C. Taballione for the guidance on the use of photonic chip.

S. C. and L.-C. P. contributed equally to this work.

*j.j.renema@utwente.nl
 †yongheng@ustc.edu.cn
 ‡whui@ustc.edu.cn
 §pan@ustc.edu.cn

- [1] E. Knill, R. Laflamme, and G. J. Milburn, *Nature (London)* **409**, 46 (2001).
- [2] P. Kok, W. J. Munro, K. Nemoto, T. C. Ralph, J. P. Dowling, and G. J. Milburn, *Rev. Mod. Phys.* **79**, 135 (2007).
- [3] J.-W. Pan, Z.-B. Chen, C.-Y. Lu, H. Weinfurter, A. Zeilinger, and M. Żukowski, *Rev. Mod. Phys.* **84**, 777 (2012).
- [4] J. L. O’Brien, *Science* **318**, 1567 (2007).
- [5] T. D. Ladd, F. Jelezko, R. Laflamme, Y. Nakamura, C. Monroe, and J. L. O’Brien, *Nature (London)* **464**, 45 (2010).
- [6] T. Rudolph, *APL Photonics* **2**, 030901 (2017).
- [7] R. Raussendorf and H. J. Briegel, *Phys. Rev. Lett.* **86**, 5188 (2001).
- [8] R. Raussendorf, D. E. Browne, and H. J. Briegel, *Phys. Rev. A* **68**, 022312 (2003).
- [9] P. Walther, K. J. Resch, T. Rudolph, E. Schenck, H. Weinfurter, V. Vedral, M. Aspelmeyer, and A. Zeilinger, *Nature (London)* **434**, 169 (2005).
- [10] H. J. Briegel, D. E. Browne, W. Dür, R. Raussendorf, and M. Van den Nest, *Nat. Phys.* **5**, 19 (2009).
- [11] D. E. Browne and T. Rudolph, *Phys. Rev. Lett.* **95**, 010501 (2005).
- [12] L.-M. Duan and R. Raussendorf, *Phys. Rev. Lett.* **95**, 080503 (2005).
- [13] K. Kieling, T. Rudolph, and J. Eisert, *Phys. Rev. Lett.* **99**, 130501 (2007).
- [14] H. A. Zaidi, C. Dawson, P. van Loock, and T. Rudolph, *Phys. Rev. A* **91**, 042301 (2015).
- [15] M. Gimeno-Segovia, P. Shadbolt, D. E. Browne, and T. Rudolph, *Phys. Rev. Lett.* **115**, 020502 (2015).
- [16] M. Pant, D. Towsley, D. Englund, and S. Guha, *Nat. Commun.* **10**, 1070 (2019).
- [17] S. Bartolucci, P. Birchall, H. Bombin, H. Cable, C. Dawson, M. Gimeno-Segovia *et al.*, *Nat. Commun.* **14**, 912 (2023).
- [18] N. H. Lindner and T. Rudolph, *Phys. Rev. Lett.* **103**, 113602 (2009).
- [19] S. E. Economou, N. Lindner, and T. Rudolph, *Phys. Rev. Lett.* **105**, 093601 (2010).
- [20] M. Gimeno-Segovia, T. Rudolph, and S. E. Economou, *Phys. Rev. Lett.* **123**, 070501 (2019).
- [21] I. Schwartz, D. Cogan, E. R. Schmidgall, Y. Don, L. Gantz, O. Kenneth, N. H. Lindner, and D. Gershoni, *Science* **354**, 434 (2016).
- [22] J. Lee, B. Villa, A. Bennett, R. Stevenson, D. Ellis, I. Farrer, D. Ritchie, and A. Shields, *Quantum Sci. Technol.* **4**, 025011 (2019).
- [23] P. Thomas, L. Ruscio, O. Morin, and G. Rempe, *Nature (London)* **608**, 677 (2022).

- [24] D. Cogan, Z.-E. Su, O. Kenneth, and D. Gershoni, *Nat. Photonics* **17**, 324 (2023).
- [25] C. K. Hong and L. Mandel, *Phys. Rev. Lett.* **56**, 58 (1986).
- [26] C. Wagenknecht, C.-M. Li, A. Reingruber, X.-H. Bao, A. Goebel, Y.-A. Chen, Q. Zhang, K. Chen, and J.-W. Pan, *Nat. Photonics* **4**, 549 (2010).
- [27] S. Barz, G. Cronenberg, A. Zeilinger, and P. Walther, *Nat. Photonics* **4**, 553 (2010).
- [28] M. Varnava, D. E. Browne, and T. Rudolph, *Phys. Rev. Lett.* **100**, 060502 (2008).
- [29] F. V. Gubarev, I. V. Dyakonov, M. Y. Saygin, G. I. Struchalin, S. S. Straupe, and S. P. Kulik, *Phys. Rev. A* **102**, 012604 (2020).
- [30] P. Senellart, G. Solomon, and A. White, *Nat. Nanotechnol.* **12**, 1026 (2017).
- [31] J. H. Weber, B. Kambs, J. Kettler, S. Kern, J. Maisch, H. Vural *et al.*, *Nat. Nanotechnol.* **14**, 23 (2019).
- [32] X. You, M.-Y. Zheng, S. Chen, R.-Z. Liu, J. Qin, M.-C. Xu *et al.*, *Adv. Opt. Photonics* **4**, 066003 (2022).
- [33] H. Wang, Y. He, Y.-H. Li, Z.-E. Su, B. Li, H.-L. Huang *et al.*, *Nat. Photonics* **11**, 361 (2017).
- [34] H. Wang, J. Qin, X. Ding, M.-C. Chen, S. Chen, X. You, Y.-M. He *et al.*, *Phys. Rev. Lett.* **123**, 250503 (2019).
- [35] C. Taballione, R. van der Meer, H. J. Snijders, P. Hooijschuur, J. P. Epping, M. de Goede *et al.*, *Mater. Quantum Technol.* **1**, 035002 (2021).
- [36] See Supplemental Material at <http://link.aps.org/supplemental/10.1103/PhysRevLett.132.130603> for detailed descriptions of single-photon source and its frequency conversion, programmable photonic chip, noise analyses, heralding efficiency and state fidelity estimation, and generation of n -GHZ states using linear optics, which includes Refs. [32,35,37–40].
- [37] X. Ding *et al.*, arXiv:2311.08347.
- [38] S. Bartolucci *et al.*, arXiv:2106.13825.
- [39] J.-P. Li *et al.*, *Phys. Rev. Lett.* **126**, 140501 (2021).
- [40] J. Zeuner, A. N. Sharma, M. Tillmann, R. Heilmann, M. Gräfe, A. Moqanaki, A. Szameit, and P. Walther, *npj Quantum Inf.* **4**, 13 (2018).
- [41] H. Wang, Y.-M. He, T.-H. Chung, H. Hu, Y. Yu, S. Chen *et al.*, *Nat. Photonics* **13**, 770 (2019).
- [42] N. Tomm, A. Javadi, N. O. Antoniadis, D. Najer, M. C. Löbl, A. R. Korsch *et al.*, *Nat. Nanotechnol.* **16**, 399 (2021).
- [43] R. Hanbury Brown and R. Twiss, *Nature (London)* **178**, 1447 (1956).
- [44] C. K. Hong, Z. Y. Ou, and L. Mandel, *Phys. Rev. Lett.* **59**, 2044 (1987).
- [45] O. Gühne and G. Tóth, *Phys. Rep.* **474**, 1 (2009).
- [46] H.-S. Zhong, Y. Li, W. Li, L.-C. Peng, Z.-E. Su, Y. Hu *et al.*, *Phys. Rev. Lett.* **121**, 250505 (2018).
- [47] N. Maring *et al.*, arXiv:2306.00874.
- [48] H. Cao, L. M. Hansen, F. Giorgino, L. Carosini, P. Zahálka, F. Zilk, J. C. Loredó, and P. Walther, following Letter, Photonic source of heralded Greenberger-Horne-Zeilinger states, *Phys. Rev. Lett.* **132**, 130604 (2024).